AIMS Agriculture and Food, 10(3): 638–661.
DOI: 10.3934/agrfood.2025032
Received: 07 July 2025
Revised: 13 August 2025
Accepted: 22 August 2025
Published: 01 September 2025

http://www.aimspress.com/journal/agriculture

Research article

The improvement of corn grain drying using air dehumidification: Energy consumption evaluation and techno-economic analysis

Dewi Qurrota A'yuni[1,2], Setia Budi Sasongko[2], Moh. Djaeni[2,*], Andri Cahyo Kumoro[2] and Agus Subagio[3]

[1] Chemical Engineering Study Program, Faculty of Industrial Technology, Institut Teknologi Sumatera, Jl. Terusan Ryacudu, Way Huwi, Jati Agung, South Lampung, 35365, Indonesia
[2] Department of Chemical Engineering, Faculty of Engineering, Universitas Diponegoro, Jl. Prof. Sudharto, SH, Tembalang, Semarang, Central Java, 50275, Indonesia
[3] Department of Physics, Faculty of Science and Mathematics, Universitas Diponegoro, Jl. Prof. Sudharto, SH, Tembalang, Semarang, Central Java, 50275, Indonesia

* **Correspondence:** Email: moh.djaeni@live.undip.ac.id; Tel: +62247460058; Fax: +62247460055.

Abstract: Freshly harvested corn contains high moisture content, thereby requiring a drying process to prevent quality degradation. This research aimed to improve the conventional drying process by adding an air dehumidification process with solid desiccant. Corn grains were dried at various temperatures (40, 50, 60, and 70 °C) and two airflow rates (10 and 15 m/s) at a 20–25 kg capacity. As indicators, the drying time required and energy consumption were evaluated. Research showed that air dehumidification was able to shorten the drying time, thereby reducing energy consumption and carbon emissions. At a low drying temperature (50 °C), air dehumidification showed a higher impact on moisture removal and shortened the drying process. Furthermore, the techno-economic aspect was evaluated. The research showed that the drying process with an adsorbent was most efficient at 40 °C and an air velocity of 15 m/s. In this condition, the benefit-to-cost ratio (B/C ratio) was 1.23, and the payback period was 1.41 years.

Keywords: air dehumidification; carbon dioxide emissions; desiccant; feasibility; grain drying

1. Introduction

Corn (*Zea mays*) is a staple food that supplies 5% of the calorie source with a consumption of more than 70 kg/capita/year in 2019 [1]. Also, it is used in other industries such as pharmaceuticals, beverages, and chemicals. In Asia, corn production reaches over 360 million tons/year [1]. To prolong storage life, corn is dried to reduce the moisture content to 15% or below [2]. Such low moisture content inhibits the growth of microbes, bacteria, and mold, thus preserving corn quality. In Indonesia, freshly harvested corn contains at least 28% moisture, indicating a need for a drying process to reduce its moisture content [3].

A direct sun drying process for 15 hours is able to reduce the moisture content in corn to the desired level (13%) [4]. Though being highly simple and affordable, using only an open tray or mat drying, the aforementioned method is weather-dependent, requires a long drying time, and can lead to product contamination. Besides requiring a long drying time, this method also needs a large area corresponding to the large product capacity. To reduce the drying time, air with higher temperature and velocity is required. The air can be heated through biomass combustion as a heat source [4]. The use of a solar-biomass hybrid dryer can reduce the moisture content by 19%–13% after 5 hours of drying. In this case, a higher initial moisture content, such as in freshly harvested corn (around 28% moisture) requires a longer drying time and higher energy consumption.

A number of convective-drying processes have been applied to corn drying. Gautam et al. performed a fluidized bed drying process [5] that could dry the product in only 60 minutes. They also evaluated the effects of temperature, capacity, airflow rate, and drying time interactions on moisture removal. The statistical analysis found an optimum condition using a fluidized bed dryer at 80 ℃, 8 m/s, and 60 minutes of operation. This process still needs further assessments in terms of energy efficiency and product quality. With an operational temperature above 70 ℃, the active substance, proteins, vitamins, and other ingredients in food or agricultural products might deteriorate. Besides, the fluidized bed dryer requires more electric power to drive the grain flowing in the drying column; hence, the total energy consumption becomes higher.

Another method is the tower-type grain drying with a grain capacity of up to 90 kg, in which the dryer is operated at high drying temperatures of 90–110 ℃ [6]. Such high temperatures not only increased the drying rate but also significantly degraded product quality. To retain the physical and chemical quality of the product, corn grains can be processed using an intermittent process [7]. The quality of corn grains can be observed for some rest periods of no heat exposure (0–16 hours). The best quality is found at the longest rest period, so that the drying process can be longer than 24 hours.

Air dehumidification with solid water adsorbents such as zeolite or silica is a potential option for corn drying. In this method, the relative humidity of ambient air as the drying medium is reduced using zeolite or silica gel. The low relative humidity can enhance the drying driving force; by doing so, drying can be conducted at low or medium temperatures, retaining vitamins, active components, and corn ingredients. Moreover, the drying process can be faster and more efficient when compared with the one without air dehumidification [8–10].

Previous studies have evaluated the effects of air dehumidification on the food drying process. A'yuni et al. [11] found that air dehumidification accelerated moisture removal, improved heat efficiency, and preserved the quality of onion bulbs. With air dehumidification, the browning process and active substance deterioration in apples were reduced compared with those exposed to heat convection drying without air dehumidification [12]. Furthermore, air dehumidification in a fluidized

bed drying significantly enhanced the drying rate without compromising head rice yield [13].

Currently, the question remains of how air dehumidification can affect the process in terms of economic value. This work discusses the enhancement of corn drying performance using air dehumidification by evaluating drying time and energy consumption, as well as conducting an economic feasibility analysis. The performance of drying with air dehumidification by natural zeolite and silica gel is evaluated and compared with the normal drying process without air dehumidification.

2. Materials and methods

2.1. Corn samples

Corn grains (*Zea mays var. indentata*) were bought in September 2023 from a local shop in Banyumanik, Semarang, Central Java. The moisture content of the corn grains was determined during the drying process using a G-WON GMK 303RS grain moisture meter with an accuracy of ± 0.5% and resolution of ± 0.1% (Seoul, Korea). The initial moisture content of corn grains was in the range of 20%–22%. Every drying process in this work used 20–25 kg of corn grains.

2.2. Solid water adsorbent (desiccant)

The process used zeolite and blue silica gel as desiccants that were provided by CV. Indrasari (Stadion Selatan Street, Semarang, Central Java, Indonesia). The natural zeolite is a mordenite with high silica zeolite with an Si/Al ratio of 6 (Figure 1), as presented in our previous study [14].

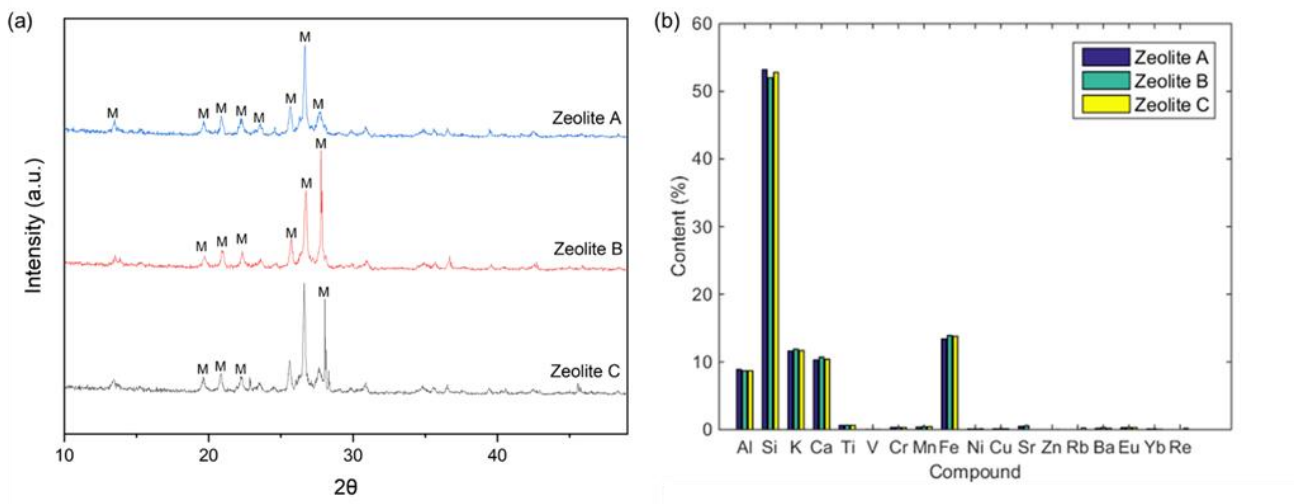

Figure 1. (a) XRD and (b) XRF analysis of zeolite used in this study.

2.3. Drying experiment

The drying process was conducted by using a vertical screw dryer, already used in a previous experiment [15]. The process began by putting 4 kg of desiccant into a drying column to dehumidify the surrounding air. Wet corn grains were then put into a feeder and circulated by a screw conveyor.

During the process, the circulated corn seeds periodically contacted with hot air at 40 ℃ and an air velocity of 10 m/s, purposely to reduce the water in the corn by evaporation. Furthermore, several thermocouple sensors were placed inside the drying column to observe the incremental temperature in the column (Figure 2). As the heat source, the LPG fuel combustion at the burner was used. During the drying process, temperature and relative humidity were measured by a temperature and humidity meter (KRISBOW KW0600561, Krisbow®, West Jakarta, Indonesia), and moisture content in corn was observed every 20 minutes. The process was terminated when the moisture content reached 15.5% or below. The drying process was repeated under these conditions: with and without desiccants at the temperatures of 50, 60, and 70 ℃ and airflows of 10 and 15 m/s. In the drying column (diameter of 0.75 m), the estimated airflow rates were 0.4 and 0.6 m/s for 10 and 15 m/s, respectively.

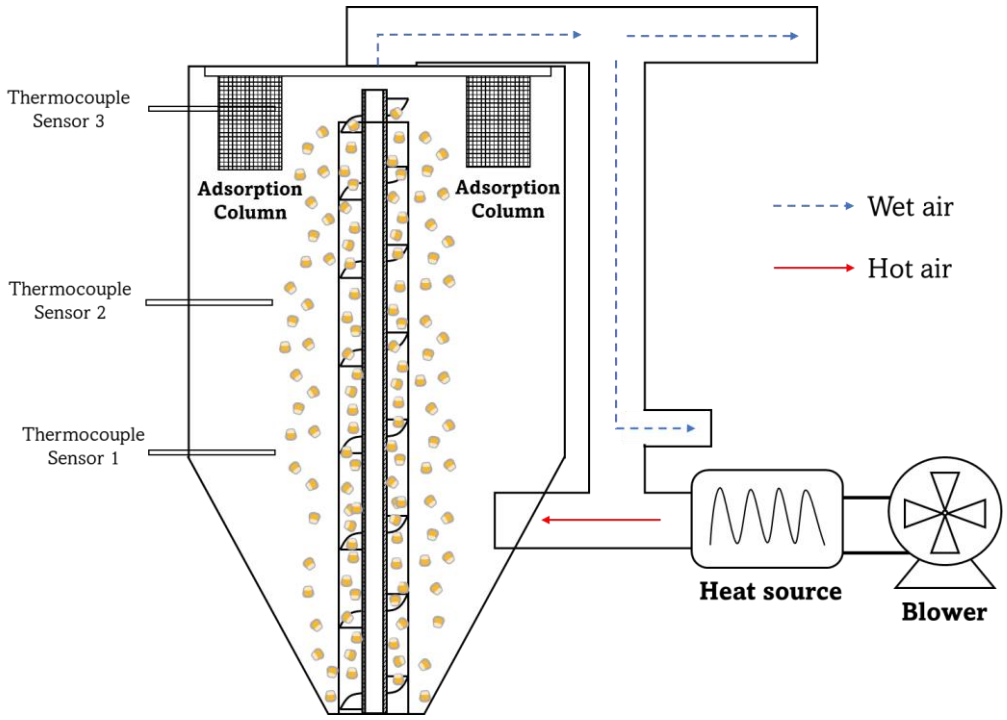

Figure 2. Schematic diagram of corn drying using a vertical dryer.

The drying rate of corn (N, kg·kg^{-1}·min^{-1}) was calculated based on the rate of moisture removal, as described by Eq (1).

$$N = \frac{(M_{t+\Delta t} - M_t)}{\Delta t} \tag{1}$$

where M_t and $M_{t+\Delta t}$ are the moisture contents at sampling times t and $t+\Delta t$.

2.4. Mathematical modeling

The moisture changes during the drying process were represented as a moisture ratio (MR, dimensionless), determined using Eq (2).

$$MR = \frac{(M_t - M_e)}{(M_0 - M_e)} \quad (2)$$

where M_0 is the initial moisture content (kg·kg^{-1}), and Me is the equilibrium moisture content (kg·kg^{-1}) that was calculated as a function of temperature (T, Kelvin) and relative humidity (RH, in decimal) as expressed in Eq (3) [16].

$$M_e = E - Fln[-(T + C)lnRH] \quad (3)$$

where E, F, and C were the grain constants of 0.34, 0.06, and 30.2, respectively. Eventually, the relationship between moisture ratio and drying time was employed to establish a mathematical model, as seen in Table 1. The models' constants were calculated using the Microsoft Excel solver (Microsoft Corp., USA).

Table 1. Mathematical models for corn drying kinetics.

Model	Equation
Newton/Lewis	$MR = \exp(-kt)$
Page	$MR = \exp(-kt^n)$
Modified-Page	$MR = \exp(-kt)^n$
Henderson-Pabis	$MR = a\exp(-kt)$
Two-term	$MR = a\exp(-k_1t) + b\exp(-k_2t)$
Verma et al.	$MR = a\exp(-kt) + (1-a)\exp(-gt)$
Midilli et al.	$MR = a\exp(-kt^n) + bt$
Diffusion approach	$MR = a\exp(-kt) + (1-a)\exp(-kbt)$

2.5. Energy consumption and energy efficiency

Specific energy consumption (SEC) was determined based on the total energy consumption for each kilogram of water evaporated (M_p). The total energy consumption consisted of heat consumption (H) and electric consumption (E). Equation (4) defines specific energy consumption.

$$SEC = \frac{H+E}{M_p}. \quad (4)$$

The electrical energy consumption was broken down into the power required for the blower (E_b) and the motor (E_m). During the drying process, the total amount of liquid petroleum gas (LPG) was used to estimate heat consumption. A heat value of LPG (47,300 kJ/kg) was applied to measure the conversion from the mass of fuel used to energy consumption. Energy efficiency (η) was also determined by energy usage, as shown in Eq (5).

$$\eta = \frac{M_p\lambda}{H + E_b + E_m} \quad (5)$$

λ refers to the latent heat of water vaporization (2429.8 kJ/kg).

2.6. Statistical analysis

Statistical analysis was used to determine the drying model parameters and the effect of three factors (condition, temperature, and airflow rate) on energy efficiency. The drying model parameters, sum of square errors (SSE), and coefficient of determination (R^2) defined the variability of the data based on several models. Those parameters were estimated using functions in Microsoft Excel (Microsoft Corporation, USA). Particularly, three-way analysis of variance (ANOVA) was used to evaluate the significance of different factors on energy efficiency. The analysis was estimated using Minitab Statistical Software (Minitab, LLC., USA).

2.7. Carbon dioxide emissions

Energy usage from this experiment was considered as a contributor to greenhouse gas emissions. To evaluate the optimum process for corn drying, this work estimated the carbon dioxide (CO_2) emission of several conditions using Eq (6) [17]

$$M_{CO_2} = \frac{\left(E \cdot EF_{CO_2eq/1kWh} + H \cdot EF_{CO_2eq/LPG}\right)}{M_p} \tag{6}$$

where M_{CO2} is the CO_2 emissions (kg) produced per kg water evaporated, and $EF_{CO_2eq/1kWh}$ and $EF_{CO_2eq/LPG}$ are the emission factors of electricity and LPG in Indonesia, i.e., 2.1×10^{-4} kg CO_2-eq./kJ and 6.54×10^{-5} kg CO_2-eq./kJ.

2.8. Techno-economic analysis

This analysis was carried out from the perspective of the user (farmer). The following assumptions were made:

a. The farmer cultivates a 10-Ha corn farm.
b. The corn is harvested at 6 tons/Ha three times a year.
c. The drying process is conducted under the conditions with the highest and lowest energy efficiencies (based on the calculation).

The techno-economic analysis involved investment, maintenance, and operational costs for dry corn production. The initial investment cost included the dryer cost, production area, supporting equipment, and others. During the corn drying process, electricity and fuel costs were calculated based on the reduction of the moisture content of the corn grains from 20.33% to 14.8%.

The techno-economic aspect was analyzed to evaluate the feasibility of the dryer by considering the break-even point (BEP), the benefit-to-cost ratio (BCR), and the payback period (PBP). The BEP was calculated using the fixed cost (C_f), product (dry corn) cost (C_{pr}), and $C_{v,pr}$ (variable cost per product) using Eq (7).

$$BEP = \frac{C_f}{(C_{product} - C_v)}. \tag{7}$$

The result of BEP indicated the minimum quantity of dry corn that must be sold to achieve profitability. Meanwhile, business feasibility was evaluated with BCR, formulated as the ratio of total

benefit and total cost of production (C_p) as in Eq (8).

$$BCR = \frac{Total\ benefit}{C_p}. \quad (8)$$

The business was considered feasible when the benefit was higher than the production cost (BCR > 1). To determine recovery time in years of the initial investment (C_i), the cash flow (S) below was included as the factor to find the payback period (Eq (9)).

$$PBP = \frac{C_i}{S}. \quad (9)$$

3. Results and discussion

3.1. Drying process

3.1.1. Effect of temperature on moisture removal

Figure 3 depicts the effects of different temperatures on corn drying using a vertical dryer. It was found that an increase in drying temperature accelerates moisture reduction. An increase by 10 ℃ (from 40 to 50 ℃) doubled the drying rate. This implies that the drying time could be reduced by half, as the latent heat of water evaporation was lower at higher temperatures and the movement of water from inside the corn tissue to the surface was faster. However, in some cases, the drying behavior did not follow the expected trend. For example, in control (Figure 3a), drying at 60 ℃ was faster than at 70 ℃. This may be attributed to the differences in initial moisture content. Another possible factor is a higher free moisture content of corn at 60 ℃, making it more easily evaporated from the corn surface. At higher temperatures, the pores of the corn surface shrank due to quick water removal, which hampered the next water transfer. Hence, the total moisture removal became slightly smaller.

Table 2. Rate of corn drying using a vertical dryer.

Airflow rate (m/s)	Temperature (℃)	Drying rate ($kg \cdot kg^{-1} \cdot min^{-1}$)		
		Control	Natural zeolite	Silica gel
10	40	0.021	0.026	0.020
	50	0.025	0.030	0.036
	60	0.039	0.040	0.037
	70	0.030	0.039	0.036
15	40	0.022	0.031	0.028
	50	0.036	0.034	0.033
	60	0.021	0.026	0.032
	70	0.038	0.043	0.038

Figure 3 also shows that moisture reduction with a desiccant was faster than without a desiccant. During drying, the desiccant continuously adsorbed air moisture, and the relative air humidity was kept low, thus enhancing the driving force for the mass transfer of water from corn to the air [18]. Yet, at

temperatures above 60 ℃, the effect of the desiccant was limited. Accordingly, in this experiment, temperatures in the range of 50–60 ℃ were considered optimum for corn drying, as confirmed in the drying rate value in Table 2.

This result contrasted with previous studies, where the highest drying rate was obtained at the highest drying temperature [19–21]. The temperature difference between the substance and the air increased with the increasing temperature used. Consequently, the drying mechanism was different for the different types of dryers and products.

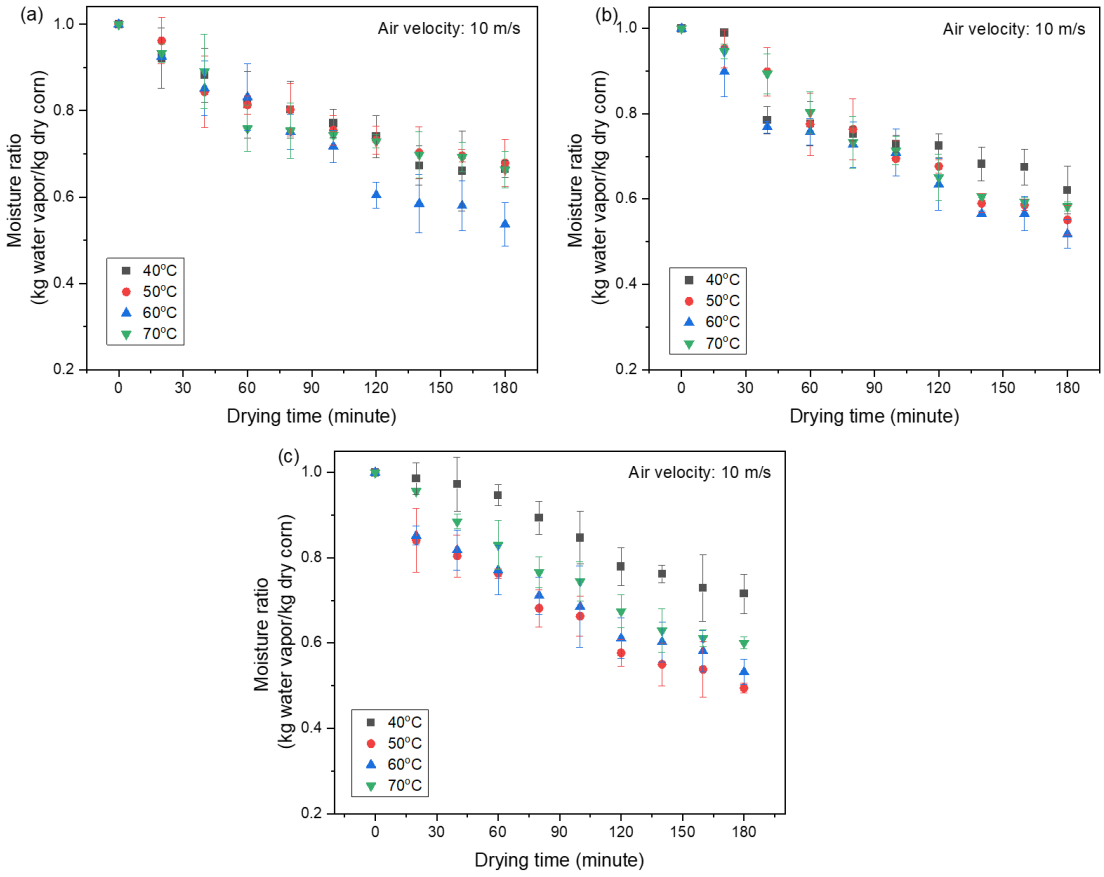

Figure 3. Moisture ratio during corn drying for (a) control, (b) natural zeolite, and (c) silica gel.

3.1.2. Effect of airflow rate

This work observed the effect of airflow rate on corn moisture removal by conducting the process at two different air velocities. Figure 4 represents the moisture ratio of corn grains during a 180-minute drying process at airflow rates of 10 and 15 m/s at different temperatures without dehumidification. Overall, higher airflow rates resulted in faster moisture reduction and increased air capacity for bringing moisture; as a result, the product could be properly dried [19]. However, based on model estimation (Figure 5), airflow rates above 11 m/s had a limited effect on moisture removal. This may be attributed to the relatively low amount of moisture in corn compared to the airflow volume (high ratio of air to product), consequently making the increase of water evaporation insignificant. A clear difference is shown at 60 ℃ (Figure 4c), indicating a lower drying rate at a higher airflow rate. In this

experiment, the initial moisture content of corn grains at 10 m/s was much higher than at 15 m/s. Therefore, at 15 m/s, corn grains have lower free moisture and higher bonding moisture. This condition limited moisture transfer from the corn surface to the surrounding air. Previous research also proved that the effect of airflow rate fluctuated at the initial stage of the drying process, particularly in the first 2 hours [22]. According to Fterich et al. [23], the influence of airflow rates on moisture reduction was lower than that of the drying temperature.

Reports on grape and rubberwood drying showed that increasing the airflow rate in the range of 1–2 m/s increased the drying rate and shortened drying time [24,25]. Authors stated that the external mass transfer increased along with the increasing airflow rate. In addition, a report from an experiment on udon drying came to the more precise conclusion that varying the airflow rate during the drying process would be more effective than maintaining a constant velocity [26]. Then, it can be assumed that the ideal airflow rate is 2 m/s during the first stage and 1 m/s during the main drying process. Research by Yan et al. [27] also demonstrated that the effect of airflow rate on moisture removal became weaker at a high airflow rate.

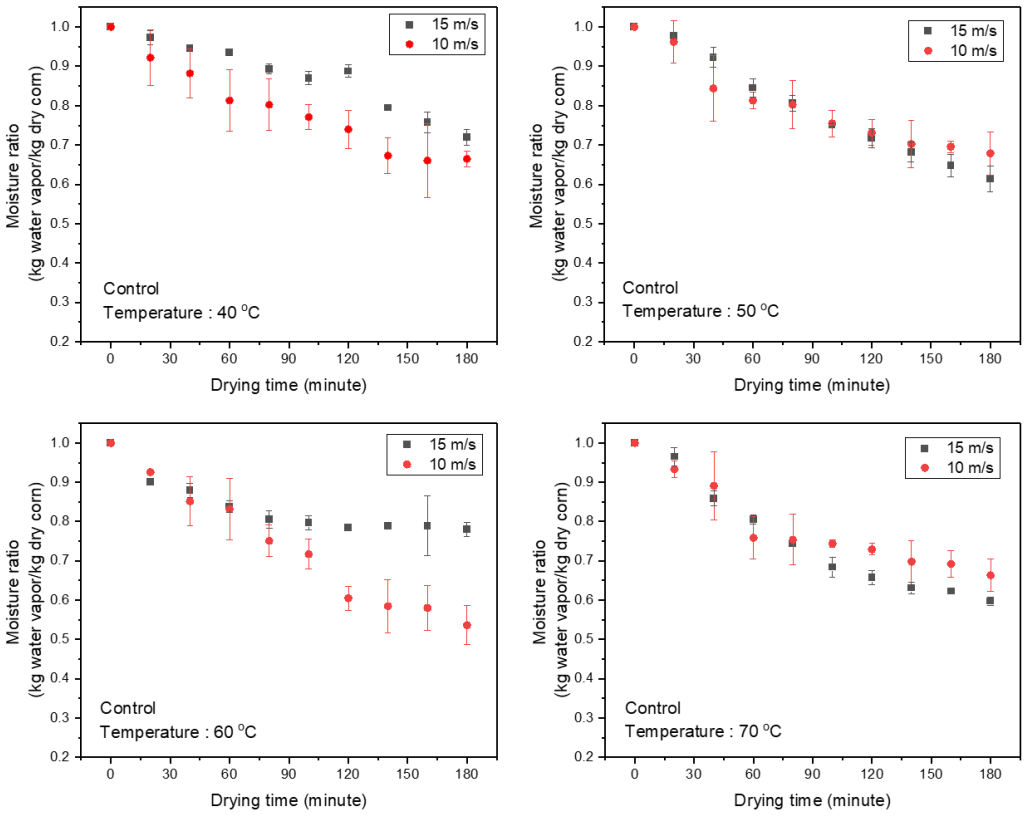

Figure 4. Moisture ratio during corn drying at different airflow rates.

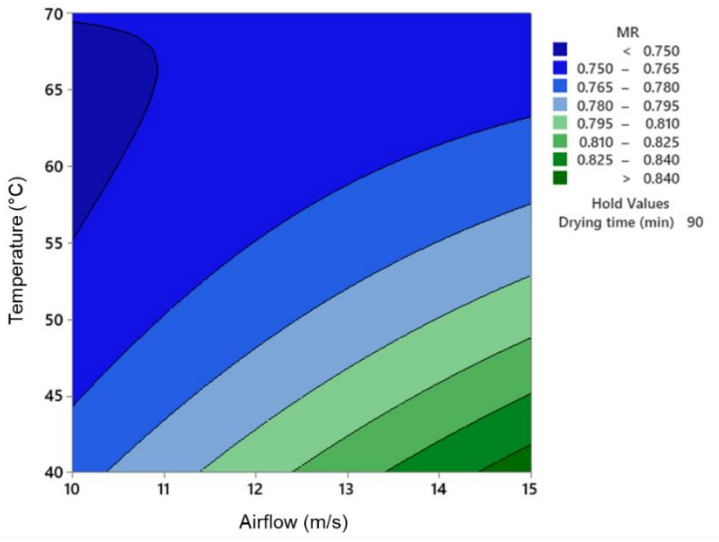

Figure 5. Effect of airflow rate and temperature on the moisture ratio of corn during the drying process.

3.1.3. Effect of air dehumidification

In this research, two solid desiccants were added to evaluate their impact on the drying process. Table 2 represents the summary of the drying rates. Overall, drying rates were elevated with the addition of air dehumidification. The objective of using air dehumidification in the drying process was to decrease the relative humidity of the air as the drying medium. As the relative humidity decreases, the pressure difference between the corn surface and the surrounding air decreases; hence, the external moisture transfer becomes larger, and the drying process becomes faster [19,21]. This relationship is shown in Figure 6, indicating that air dehumidification reduces relative humidity and thus decreases the equilibrium moisture content of corn grains.

Figure 7 shows the curve of moisture reduction during the drying process under air dehumidification. Zeolite showed a superior effect on moisture reduction at the operational temperature of 40 ℃. Zeolite and silica showed different phenomena in water affinity. Zeolite depicted a Type I adsorption based upon IUPAC classification, while silica possessed a linear-type adsorption (the higher the relative humidity, the higher the water-loading capacity). In this case, for a lower relative humidity, the ability of zeolite to adsorb water was still high and stable. At a lower operational temperature (40 ℃), the evaporation rate of moisture from corn to air was slow, thus reducing the air humidity in the drying chamber. The water adsorption to silica was also consequently reduced [28]. However, limited water vapor adsorption was also found at a high temperature (70 ℃ or higher) due to the low relative air humidity. In such conditions, the existing desiccant was no longer required [29].

Based on several research works, desiccants can uptake approximately 0.07–0.14 g of H_2O/g dry zeolite and 0.03–0.30 g of H_2O/g dry silica gel [30,31]. The decrease in relative humidity depends on the adsorption capacity or water uptake of the desiccant. Once zeolite or silica gel adsorbs more water vapor from the air, the surrounding moisture content is much lower, and the relative humidity is significantly lower.

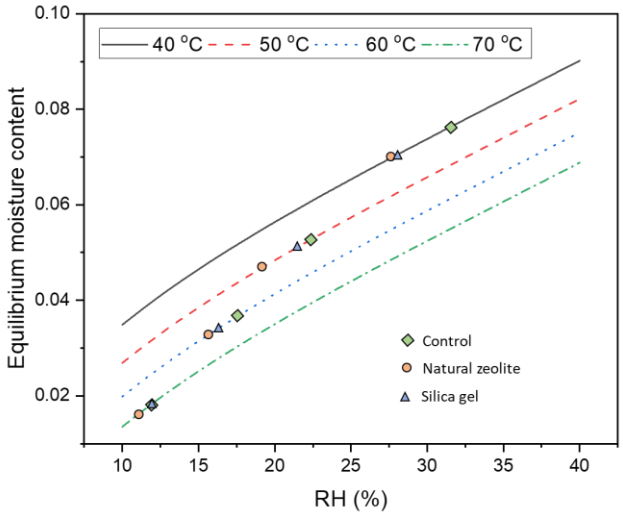

Figure 6. Equilibrium moisture content of corn at different temperatures and relative humidity (RH).

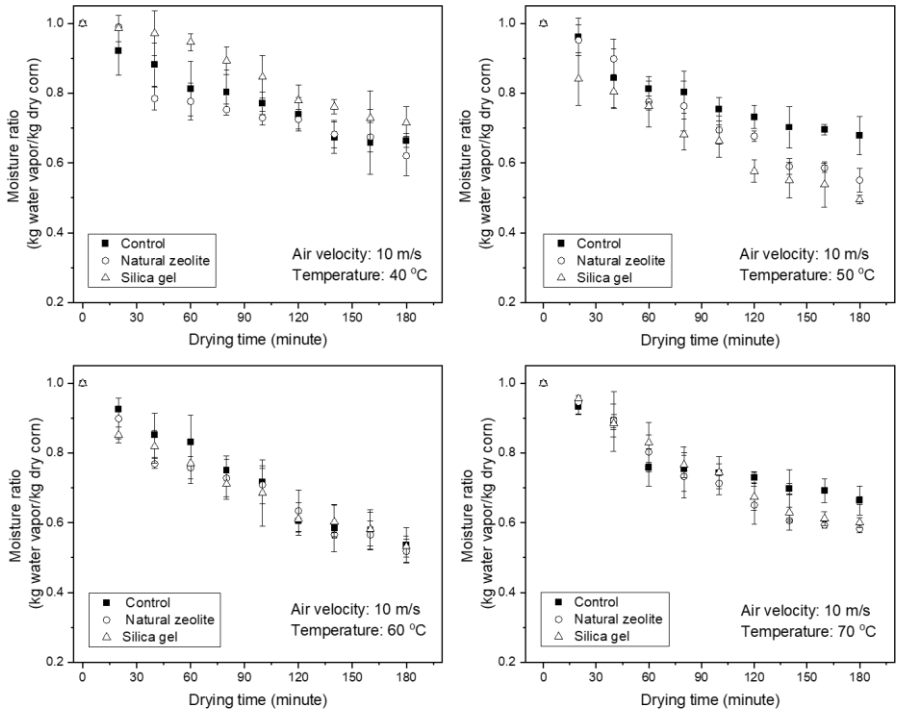

Figure 7. Moisture ratio during corn drying using different desiccants.

3.1.4. Mathematical models of the drying process

Moisture changes in the corn drying process under different conditions were examined by

mathematical models of thin-layer drying. The parameters of the models are displayed in Table 3. More detailed values, including models' constants and parameters at different drying temperatures and airflow rates, are summarized in the Supplementary Tables S1–S3. These models were used to describe the drying kinetics at different temperatures and airflow rates with the use of different desiccants. The most suitable model was selected based on the statistical parameters, namely the sum of squares error (SSE) and coefficient of determination (R^2). The model with the lowest SSE (closest to 0) and highest R^2 (closest to 1) was then selected to predict moisture changes during the corn drying process.

As seen in Table 3, the two-term, Verma et al., and Midilli et al. models described the corn drying kinetics using a vertical dryer better than the other models. In contrast, the Newton model was the least suitable model, as shown by its low R^2 and largest SSE. Based on the most suitable model (Verma et al.), the predicted moisture ratio was calculated and compared with the experimental data, as seen in Figure 8. This is consistent with a corn drying experiment using a solar bubble dryer (SBD) [32]. That research explained that this model was developed from the two-term model, indicating a high occurrence of liquid diffusion in the moisture transfer mechanism. In addition, the first and second terms of the model represented the final and initial drying process, respectively [32]. Based on the experiment and mathematical model, the drying mechanism is described in Figure 9. Other sources found that the Midilli model was very suitable for demonstrating the corn drying process in a laboratory-scale grain dryer [6], and the Page and Lewis model had a very good correlation with corn drying in a mixed flow dryer [16].

Table 3. Calculated values of several models of corn drying.

Model	Parameter	Condition			Average
		Control	Zeolite	Silica gel	
Newton	R^2	0.9587	0.9482	0.9511	0.9527
	SSE	0.0041	0.0156	0.0077	0.0091
Page	R^2	0.9637	0.9414	0.9697	0.9583
	SSE	0.0016	0.0026	0.0013	0.0018
Modified-Page	R^2	0.9582	0.9535	0.9525	0.9547
	SSE	0.0042	0.0028	0.0048	0.0039
Henderson & Pabis	R^2	0.9629	0.9508	0.9483	0.9540
	SSE	0.0022	0.0062	0.0055	0.0046
Two-term	R^2	0.9629	0.9656*	0.9726	0.9670
	SSE	0.0012	0.0019	0.0010	0.0014
Verma et al.	R^2	0.9701	0.9652	0.9752*	0.9702
	SSE	0.0007	0.0019	0.0008**	0.0011
Midilli et al.	R^2	0.9730*	0.9530	0.9752	0.9671
	SSE	0.0007**	0.0018**	0.0009	0.0011
Diffusion approach	R^2	0.9717	0.9549	0.9711	0.9659
	SSE	0.0007	0.0034	0.0017	0.0019

Note: *Highest R^2, **Lowest SSE.

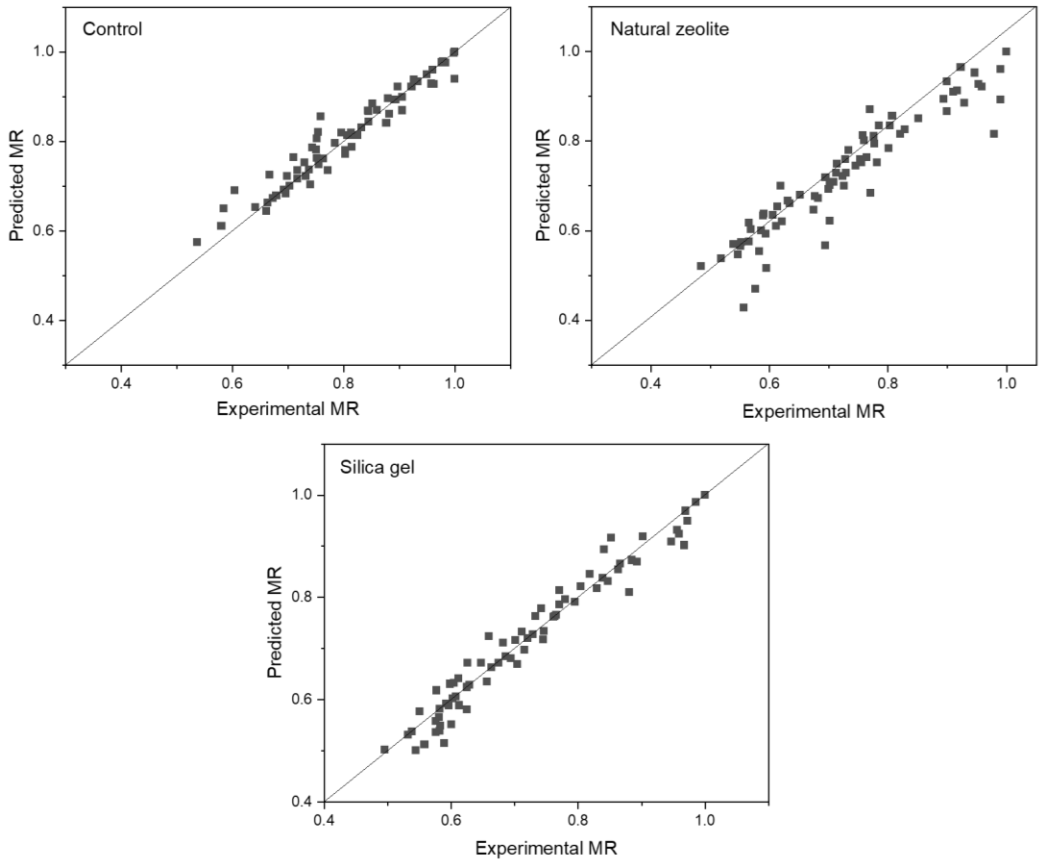

Figure 8. Comparison of experimental and predicted moisture ratio (MR) of corn drying.

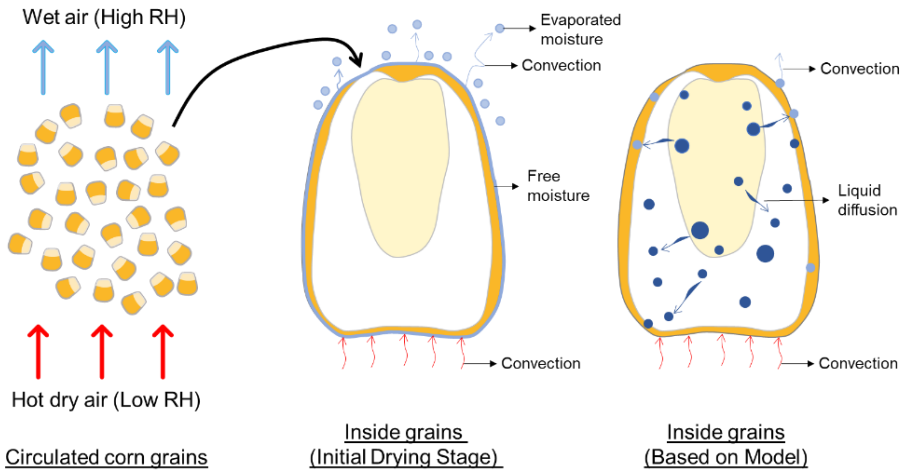

Figure 9. Mechanism of corn drying based on the experiment and mathematical model.

The drying rate constant (k) was also determined from the model regression (Tables S1–S3). The drying rate seemed to fluctuate with changes in temperature and airflow rate. However, most of the drying constant rates of dehumidification were higher than those of the conventional drying process.

For instance, at 70 ºC and an airflow rate of 15 m/s, the drying rate constants were 0.0026, 0.0034, and 0.0037 for control, natural zeolite, and silica gel dehumidification drying, respectively. Furthermore, the energy analysis confirmed the interaction between factors and responses, not only limited to the drying rate.

3.2. Energy consumption

The drying process was conducted using a vertical dryer at different temperatures and airflow rates. Total energy consumption was calculated according to heat and electricity consumption. Heat consumption was measured with the total LPG mass used during the drying process, and electricity was based on the power needed for the blower and screw motor. In this work, energy consumption is represented as specific energy consumption (Figure 10) and energy efficiency (Figure 11). As seen in Figure 10, energy consumption increased with increasing airflow rate. A similar result was also found in potato processing using a convective dryer at several air velocities [33]. However, in the case of temperature, energy consumption was not always higher at higher temperatures. It was found that processing at 60 ℃ consumed more energy than at other temperatures, especially for the control and natural zeolite dehumidification process. Such different effects of temperature were also found in previous research [33–35]. Golpour et al. [33] reported that raising temperature and airflow rate had increased the specific energy consumption of convective drying.

The additional heat and electricity requires a larger energy supply and causes an increase in energy consumption. In contrast, El-Mesery [34] succeeded in decreasing energy consumption at higher temperatures and lower airflow rates due to a short period of drying time. Meanwhile, research by Macedo et al. [35] observed that between temperatures of 40 and 80 ℃, the largest energy consumption was found under 60 ℃. In other words, specific energy consumption is determined by the moisture removal as a result of the interaction of temperature, airflow rate, and drying time. In this work, the insignificant impact of increasing temperature and airflow rate on moisture removal made the energy consumption lower at low temperatures.

For all processes, the drying process without air dehumidification consumed more energy. Its consumption was in the range of 37–103 MJ/kg water evaporated, with the highest occurring at 60 and 15 m/s. Using desiccants for air dehumidification, the maximum energy consumption was reduced by 50% to about 54 and 51 MJ/kg water evaporated for natural zeolite and silica gel, respectively. The lowest specific energy consumption, 20 MJ/kg at 40 ℃ and 15 m/s, describes the minimum energy required to evaporate 1 kg of moisture from the corn. Smaller energy consumption (1–8 MJ/kg) was obtained when the corn was processed using an industrial horizontal dryer with natural gas as the heat source [36]. Another study reported a higher energy consumption of corn drying powered by exhaust waste heat, about 468–529 MJ/kg [37]. In laboratory-scale potato drying, the specific energy consumption was also higher (194–314 MJ/kg) at an airflow rate of 0.5–1.5 m/s and temperatures of 40–70 ℃ [33]. Energy consumption could be higher or lower depending on the heat source of the drying process. To make it clearer, compared to an electric heater, the use of butane gas in a convective drying process could save 75% more energy consumption [34]. Hence, changing the heat source can also affect the CO_2 production from the drying process [38].

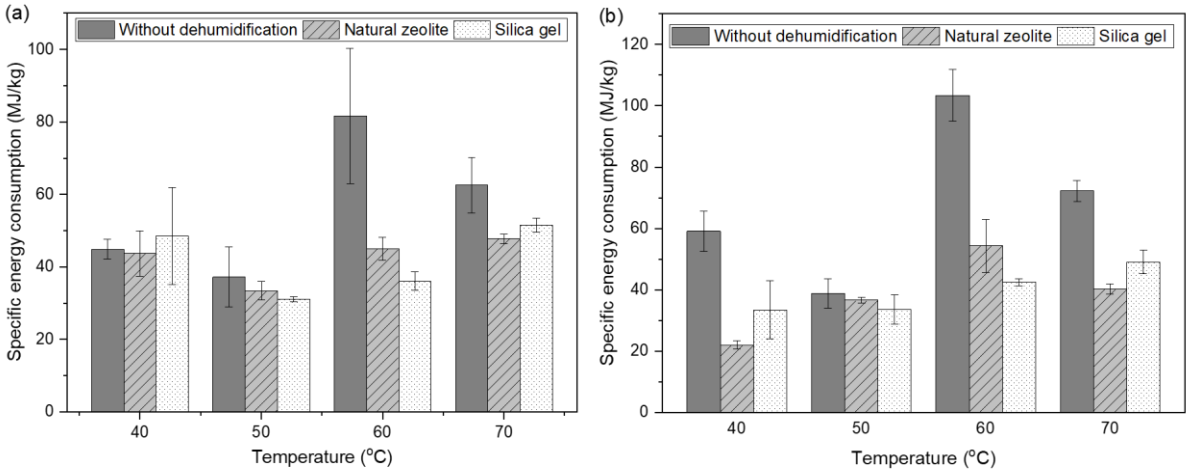

Figure 10. Specific energy consumption of the corn drying process under different conditions at airflow rates of (a) 10 m/s and (b) 15 m/s.

Energy efficiency was evaluated based on a 3-hour drying process. It is important to note that after the experiment, some corn was successfully dried, but others were not. Figure 11 shows the effect of temperature, airflow rate, and dehumidification on energy efficiency. It can be seen that energy efficiency was increased by increasing the airflow rate, with the highest at 40 ℃ and 15 m/s with zeolite dehumidification. Also, dehumidification had a positive impact on energy efficiency due to the shorter drying time and lower energy consumption. Otherwise, raising the temperature to above 50 ℃ had a negative effect on energy efficiency.

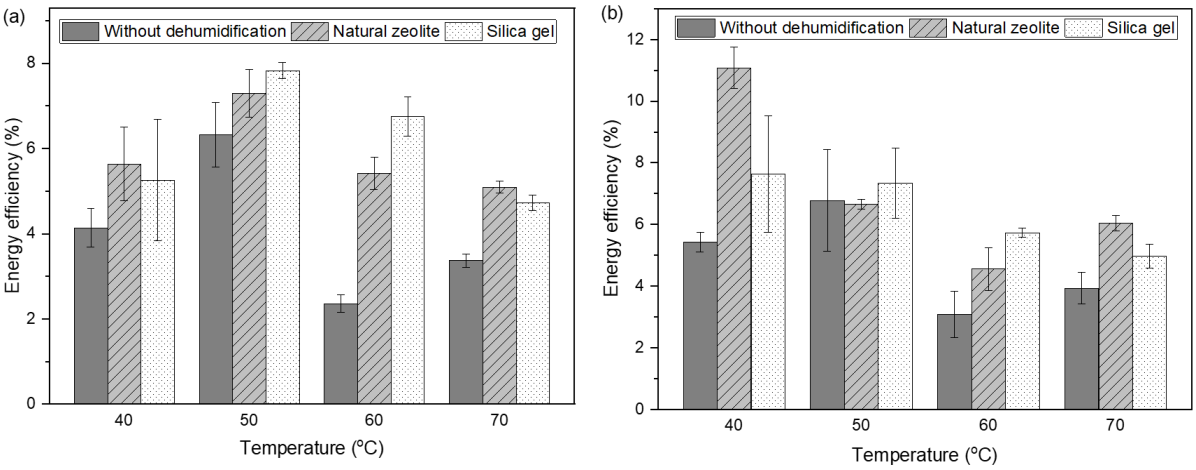

Figure 11. Energy efficiency of corn drying under different conditions at airflow rates of (a) 10 m/s and (b) 15 m/s.

This result showed that the maximum energy efficiency in this experiment was about 11%, lower than previous research using a rotary dryer [38], mixed flow dryer [39], and convective tray dryer [40],

and higher than solar indirect dryers [41,42]. An alternative method to increase energy efficiency is loading more product into the drying process. Hence, more moisture will evaporate from the product with an equal amount of input energy. Previously, it was proved that increasing the drying capacity from 10 to 40 kg could raise energy efficiency two-fold [38]. The significance of the three variables was evaluated by three-way ANOVA, as displayed in Table 4. All sources had a significant impact on energy efficiency, except the airflow rate factor. This occurred due to the limitation of using only two airflow rate values. For further analysis of the effect of the airflow rate, observations should include a wider range of airflow rates.

Table 4. Three-way ANOVA of different factors in the corn drying process using a vertical dryer.

Sources	DoF	Sum of squares	Mean square	F value	P value**
Dehumidification	2	0.0064	0.0032	54.82	<0.0001
Airflow rate	1	0.0001	0.0001	1.071	0.3058
Temperature	3	0.0086	0.0029	48.98	<0.0001
Dehumidification*Airflow rate	2	0.0009	0.0005	8.305	0.0008
Dehumidification*Temperature	6	0.0035	0.0006	9.841	<0.0001
Airflow rate* Temperature	3	0.0021	0.0007	12.06	<0.0001
Dehumidification*Airflow rate *Temperature	6	0.0020	0.0003	5.568	0.0002
Dehumidification*Airflow rate *Temperature	23	0.0237	0.0010	17.52	<0.0001
Error	48	0.0028	0.0001		
Model	71	0.0265			

Note: **Significant at P value < 0.05.

3.3. Carbon dioxide emissions

The environmental emissions of corn drying were estimated based on the energy consumption during the process. As presented in Figure 12, the highest CO_2 emission was observed at the drying process without air dehumidification, ranging from 4.0 to 12.8 kg CO_2-eq./kg water vapor. This high emission was associated with high drying temperatures and long drying times. In contrast, for air dehumidification drying, increasing the airflow rate had no significant impact on CO_2 emissions, which remained in the range of 2.7–5.0 kg CO_2-eq./kg water vapor. This result showed that the application of air dehumidification reduced greenhouse gas emissions by more than 70%. The significant reduction in CO_2 emissions follows the specific energy consumption, as shown in Figure 12, confirming the effectiveness of air dehumidification drying. A similar result was observed in rice drying using a rotary dryer (without air dehumidification) that produced 0.9–6.0 kg CO_2-eq./kg water vapor [38]. Much higher emissions were found in green peas drying using various methods, particularly in convective drying at 40 ℃ due to its low thermal efficiency [43].

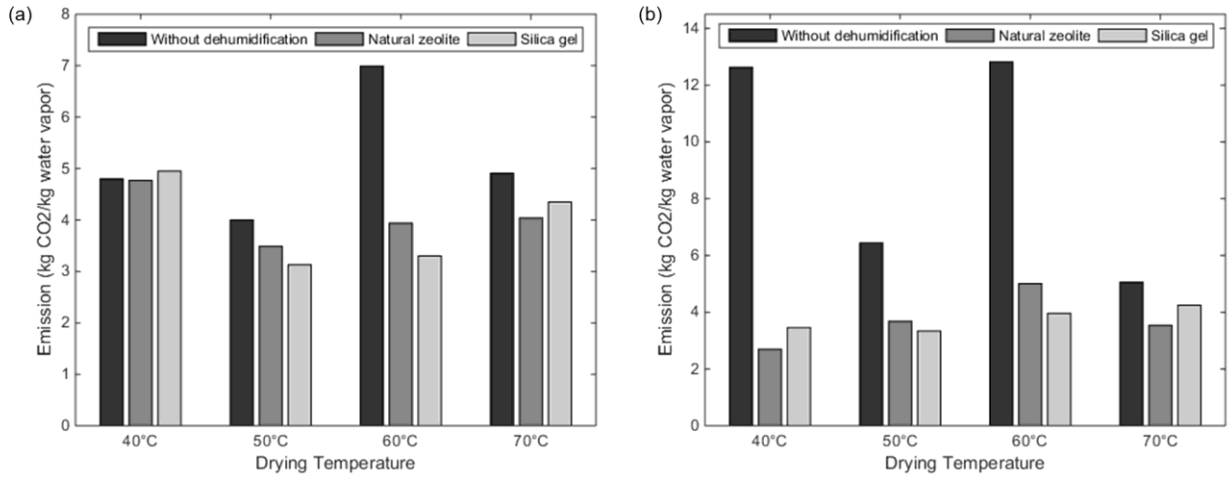

Figure 12. CO_2 emissions of the corn drying process at (a) 10 m/s and (b) 15 m/s.

Table 5. Indicators in the techno-economic analysis.

		Zeolite, 40 ºC, 15 m/s	Control, 60 ºC, 15 m/s
1.	Initial investment (USD)	15,428.11	15,428.11
2.	Loading capacity (kg/batch)	500	500
3.	Dried corn production (kg/year)	168,317	168,380
4.	Interest (%)	3	3
5.	Depreciation (%)	10	10
6.	Fuel cost (USD/dryer)	9.87	130.68
7.	Labor cost (USD/dryer)	7.42	7.42
8.	Annual fixed cost (USD)	4675.39	4675.39
9.	Annual variable cost (USD)	45,860.01	89,545.63
10.	Selling price of dried corn (USD/kg)	0.37	0.59
11.	BEP (kg)	47,225	73,680
12.	BCR	1.23	1.06
13.	PBP (year)	1.41	3.14

3.4. Techno-economic analysis

Following the assumption that the drying process is conducted under the condition with the highest and lowest energy efficiencies, this analysis was only examined for the dehumidification drying using a natural zeolite desiccant at 40 ℃ and an airflow rate of 15 m/s, and the control at 60 ℃ and an airflow rate of 15 m/s (Table 5). The initial investment included the dryer cost, area of production, production cost, and other costs to support the dry corn production. The total annual investment of the vertical dryer was USD 12,568.38, with a total production of more than 168,000 dry corn/year. The significant difference between natural zeolite and control was in fuel consumption. According to the experiment, using air dehumidification, fuel consumption can be reduced by 93%. Therefore, the cost of dry corn is much lower after being processed with the assistance of natural

zeolite (USD 0.37/kg). To recover the investment (PBP), it is necessary to operate the drying method for 1.41 and 3.14 years for natural zeolite and control, respectively. Using natural zeolite, the PBP is similar to a corn crossflow column drying with a drying charge of USD 0.007/kg [44]. A report compared the economic aspects of low-temperature grain drying under several conditions and capacities [45]. According to the estimation, the drying system was more feasible at a large capacity and profitable when utilizing the grain residues as fuel. Also, the use of biomass such as rice husk significantly decreased the carbon dioxide emissions of the drying process. The result of BCR indicated that this business is feasible or flexible to carry out a net cash flow greater than the investment, as it exceeds the value of 1.

4. Conclusions

The corn drying process with air dehumidification using silica gel and natural zeolite was studied. This research also observed the effects of different temperatures and airflow rates. It was observed that the optimum drying temperature was different under different conditions. For the control process (without air dehumidification), the process with natural zeolite, and that with silica gel, the highest moisture removal occurred at 70, 60, and 50 ℃, respectively. At a higher temperature, moisture reduction was highly determined by temperature rather than by air dehumidification. Based on the results, it can be summarized that drying of 20–25 kg of corn requires a 2–3 hour drying process after the addition of desiccant for air dehumidification. The model was also studied with suitable parameter estimation. Based upon the total energy consumption and carbon emissions during the drying process, it was estimated that air dehumidification decreased the specific energy consumption, increased energy efficiency, and reduced carbon emissions. The techno-economic evaluation indicates that this experiment is feasible to adopt.

Author contributions

Dewi Qurrota A'yuni: Visualization, Investigation, Methodology, Writing–original draft, Writing–review & editing; Setia Budi Sasongko: Data curation, Methodology, Formal analysis; Moh. Djaeni: Conceptualization, Supervision, Validation, Writing–review & editing; Andri Cahyo Kumoro: Validation, Writing–review & editing; Agus Subagio: Resources, Supervision, Validation. All authors have read and agreed to the published version of the manuscript.

Use of Generative-AI tools declaration

The authors declare they have not used Artificial Intelligence (AI) tools in the creation of this article.

Acknowledgments

This research was Funded by Universitas Diponegoro 2025.

Conflict of interest

There is no conflict of interest.

References

1. Erenstein O, Jaleta M, Sonder K, et al. (2022) Global maize production, consumption and trade: trends and R&D implications. *Food Sec* 14: 1295–1319. https://doi.org/10.1007/s12571-022-01288-7
2. Codex Alimentarius International Food Standard (2019) Standard for Maize (Corn). Available from: https://www.fao.org/fao-who-codexalimentarius/sh-proxy/en/?lnk=1&url=https%253A%252F%252Fworkspace.fao.org%252Fsites%252Fcodex%252FStandards%252FCXS%2B153-1985%252FCXS_153e.pdf.
3. Badan Pusat Statistik-Statistics Indonesia (2024) Maize Harvested Area and Production in Indonesia 2023. Available from: https://www.bps.go.id/en/publication/2024/08/16/fa2d1e4d5414f76a9bc3c713/maize-harvested-area-and-production-in-indonesia-2023.html.
4. Akowuah JO, Bart-Plange A, Dzisi KA (2021) Thin layer mathematical modelling of white maize in a mobile solar-biomass hybrid dryer. *Res Agric Eng* 67: 74–83. https://doi.org/10.17221/56/2020-RAE
5. Gautam S, Gautam A, Mahant B, et al. (2021) A Statistical optimization of convective Drying of corn kernels in a fluidized bed dryer. *J Eng Res* 11: 30–40. https://doi.org/10.36909/jer.10775
6. Çelik E, Parlak N, Çay Y (2021) Experimental and numerical study on drying behavior of CORN grain. *Heat Mass Transfer* 57: 321–332. https://doi.org/10.1007/s00231-020-02954-2
7. Mabasso GA, Siqueira VC, Quequeto WD, et al. (2022) Microscopy of maize grains subjected to continuous and intermittent drying. *Acta Sci. Agro.* 44: e54906–e54906. https://doi.org/10.4025/actasciagron.v44i1.54906
8. Konopatzki EA, Christ D, Coelho SRM, et al. (2022) Coffee dryer with dehydrated air: A technical and economic viability analysis. *Eng Agríc* 42: e20210003. https://doi.org/10.1590/1809-4430-Eng.Agric.v42n4e20210003/2022
9. Su M, Han X, Dai Y, et al. (2024) Investigation on recirculated regenerative solid desiccant-assisted dehumidification system: Impact of system configurations and desiccant materials. *Energy* 286: 129629. https://doi.org/10.1016/j.energy.2023.129629
10. Hanif S, Sultan M, Miyazaki T, et al. (2019) Investigation of energy-efficient solid desiccant system for wheat drying. *Int J Agr Bio Eng* 12: 221–228. https://doi.org/10.25165/j.ijabe.20191201.3854
11. A'yuni DQ, Djaeni M, Asiah N, et al. (2022) Enhancement of onion bulb drying with air dehumidification assisted dryer. *AIMS Agric Food* 7: 168–183. http://www.aimspress.com/article/doi/10.3934/agrfood.2022011
12. Matys A, Wiktor A, Dadan M, et al. (2021) Influence of Ultrasound and the Conditions of Convective Drying with Dehumidified Air on the Course of the Process and Selected Properties of Apple Tissue. *Foods* 10: 1840. https://doi.org/10.3390/foods10081840
13. Luthra K, Sadaka S (2019) Effects of air dehumidification on the performance of a fluidized bed dryer and the rice quality, 2019 ASABE Annual International Meeting, 1900322. https://doi.org/10.13031/aim.201900322
14. A'yuni DQ, Hadiantono H, Velny V, et al. Effect of Potassium Hydroxide Concentration and Activation Time on Rice Husk-Activated Carbon for Water Vapor Adsorption. *Iran J Mater Sci Eng* 21: 82–91. https://doi.org/10.22068/ijmse.3522

15. Utari FD, Yasintasia C, Ratridewi M, et al. (2022) Evaluation of paddy drying with vertical screw conveyor dryer (VSCD) at different air velocities and temperatures. *Chem Eng Process* 174: 108881. https://doi.org/10.1016/j.cep.2022.108881
16. Mondal MdHT, Akhtaruzzaman Md, Sarker MdSH (2022) Modeling of dehydration and color degradation kinetics of maize grain for mixed flow dryer. *J Agric Food Res* 9: 100359. https://doi.org/10.1016/j.jafr.2022.100359
17. El Hage H, Herez A, Ramadan M, et al. (2018) An investigation on solar drying: A review with economic and environmental assessment. *Energy* 157: 815–829. https://doi.org/10.1016/j.energy.2018.05.197
18. Djaeni M, A'yuni DQ, Alhanif M, et al. (2021) Air dehumidification with advance adsorptive materials for food drying: A critical assessment for future prospective. *Dry Technol* 39: 1648–1666. https://doi.org/10.1080/07373937.2021.1885042
19. Namkanisorn A, Murathathunyaluk S (2020) Sustainable drying of galangal through combination of low relative humidity, temperature and air velocity. *Energy Rep* 6: 748–753. https://doi.org/10.1016/j.egyr.2019.11.150
20. Charmongkolpradit S, Somboon T, Phatchana R, et al. (2021) Influence of drying temperature on anthocyanin and moisture contents in purple waxy corn kernel using a tunnel dryer. *Case Stud Therm Eng* 25: 100886. https://doi.org/10.1016/j.csite.2021.100886
21. Abasi S, Minaei S, Khoshtaghaza MH (2017) Effect of desiccant system on thin layer drying kinetics of corn. *J Food Sci Technol* 54: 4397–4404. https://doi.org/10.1007/s13197-017-2914-z
22. Chandramohan VP (2018) Influence of air flow velocity and temperature on drying parameters: An experimental analysis with drying correlations. *IOP Conf Ser: Mater Sci Eng* 377: 012197. https://doi.org/10.1007/10.1088/1757-899X/377/1/012197
23. Fterich M, Ibrahim Elamy M, Touti E, et al. (2023) Experimental and numerical study of tomatoes drying kinetics using solar dryer equipped with PVT air collector. *Eng Sci Technol, Int J* 47: 101524. https://doi.org/10.1016/j.jestch.2023.101524
24. EL-Mesery HS, Tolba NM, Kamel RM (2023) Mathematical modelling and performance analysis of airflow distribution systems inside convection hot-air dryers. *Alex Eng J* 62: 237–256. https://doi.org/10.1016/j.aej.2022.07.027
25. Chanpet M, Rakmak N, Matan N, et al. (2020) Effect of air velocity, temperature, and relative humidity on drying kinetics of rubberwood. *Heliyon* 6: e05151. https://doi.org/10.1016/j.heliyon.2020.e05151
26. Inazu T, Iwasaki K, Furuta T (2003) Effect of air velocity on fresh Japanese noodle (Udon) drying. *LWT - Food Sci Technol* 36: 277–280. https://doi.org/10.1016/S0023-6438(02)00185-8
27. Yan Y, Jiangli P, Jixian D, et al. (2022) Study on Paper Drying Rate Based on Lattice Boltzmann Method. *J Korea TAPPI* 54: 10–17. https://doi.org/10.7584/JKTAPPI.2022.2.54.1.10
28. Sultan M, Miyazaki T, Koyama S (2018) Optimization of adsorption isotherm types for desiccant air-conditioning applications. *Renew Energ* 121: 441–450. https://doi.org/10.1016/j.renene.2018.01.045
29. Djaeni M, Perdanianti AM (2019) The study explores the effect of onion (allium cepa l.) drying using hot air dehumidified by activated carbon, silica gel and zeolite. *J Phys: Conf Ser* 1295: 012025. https://doi.org/10.1088/1742-6596/1295/1/012025

30. Wahono SK, Suwanto A, Prasetyo DJ, et al. (2019) Plasma activation on natural mordenite-clinoptilolite zeolite for water vapor adsorption enhancement. *Appl Surface Sci* 483: 940–946. https://doi.org/10.1016/j.apsusc.2019.04.033
31. Xia ZZ, Chen CJ, Kiplagat JK, et al. (2008) Adsorption Equilibrium of Water on Silica Gel. *J Chem Eng Data* 53: 2462–2465. https://doi.org/10.1021/je800019u
32. Asemu AM, Habtu NG, Delele MA, et al. (2020) Drying characteristics of maize grain in solar bubble dryer. *J Food Process Eng* 43: e13312. https://doi.org/10.1111/jfpe.13312
33. Golpour I, Kaveh M, Chayjan RA, et al. (2020) Energetic and exergetic analysis of a convective drier: A case study of potato drying process. *Open Agric* 5: 563–572. https://doi.org/10.1515/opag-2020-0058
34. EL-Mesery HS (2022) Improving the thermal efficiency and energy consumption of convective dryer using various energy sources for tomato drying. *Alex Eng J* 61: 10245–10261. https://doi.org/10.1016/j.aej.2022.03.076
35. Macedo LL, Vimercati WC, Da Silva Araújo C, et al. (2020) Effect of drying air temperature on drying kinetics and physicochemical characteristics of dried banana. *J Food Process Eng* 43: e13451. https://doi.org/10.1111/jfpe.13451
36. Ünal F (2021) Energy and exergy analysis of an industrial corn dryer operated by two different fuels. *Int J Exergy* 34: 475–491. https://doi.org/10.1504/IJEX.2021.114095
37. Ononogbo C, Nwufo OC, Nwakuba NR, et al. (2021) Energy parameters of corn drying in a hot air dryer powered by exhaust gas waste heat: An optimization case study of the food-energy nexus. *Energy Nexus* 4: 100029. https://doi.org/10.1016/j.nexus.2021.100029
38. A'yuni DQ, Kurniawan D, Prayoga MPI, et al. (2024) Energy and carbon dioxide emission analysis of a batch-mode paddy drying process in a rotary dryer. *Res Agric Eng* 70: 35–42. https://doi.org/10.17221/32/2023-RAE
39. Mondal MdHT, Hossain MdA, Sheikh MdAM, et al. (2021) Energetic and exergetic investigation of a mixed flow dryer: A case study of maize grain drying. *Dry Technol* 39: 466–480. https://doi.org/10.1080/07373937.2019.1709077
40. Argo BD, Ubaidillah U (2020) Thin-layer drying of cassava chips in multipurpose convective tray dryer: Energy and exergy analyses. *J Mech Sci Technol* 34: 435–442. https://doi.org/10.1007/s12206-019-1242-9
41. Hssaini L, Ouaabou R, Hanine H, et al. (2021) Kinetics, energy efficiency and mathematical modeling of thin layer solar drying of figs (Ficus carica L.). *Sci Rep* 11: 21266. https://doi.org/10.1038/s41598-021-00690-z
42. Fantasse A, Lakhal EK, Idlimam A, et al. (2021) Energy Efficiency of Drying Kinetics Process of Hydroxide Sludge Wastes in an Indirect Convection Solar Dryer. *J Sol Energy Eng* 143: 041007. https://doi.org/10.1115/1.4049622
43. Kaveh M, Abbaspour-Gilandeh Y, Nowacka M (2021) Comparison of different drying techniques and their carbon emissions in green peas. *Chem Eng Process* 160: 108274. https://doi.org/10.1016/j.cep.2020.108274
44. Obeng-Akrofi G, Akowuah JO, Maier DE, et al. (2021) Techno-Economic Analysis of a Crossflow Column Dryer for Maize Drying in Ghana. *Agriculture* 11: 568. https://doi.org/10.3390/agriculture11060568
45. Santana PA, Lopes D de C, Neto AJS (2019) Economic analysis of low-temperature grain drying. *Emir J Food Agric* 31: 930–936. https://doi.org/10.9755/ejfa.2019.v31.i12.2040

Supplementary Data

Table S1. Calculated values of several models of corn drying without desiccant.

Model		15 m/s				10 m/s				Average
		40 ℃	50 ℃	60 ℃	70 ℃	40 ℃	50 ℃	60 ℃	70 ℃	
Newton	k	0.0011	0.0012	0.0009	0.0011	0.0025	0.0019	0.0031	0.0023	
	R^2	0.9745	0.9877	0.9750	0.9524	0.9806	0.9331	0.9699	0.8965	0.9587
	SSE	0.0020	0.0086	0.0018	0.0127	0.0005	0.0030	0.0020	0.0025	0.0041
Page	k	0.0003	0.0003	0.0002	0.0003	0.0015	0.0017	0.0017	0.0033	
	n	1.1952	1.4751	1.3174	1.3862	1.1118	1.0489	1.1395	0.9277	
	R^2	0.9821	0.9794	0.9779	0.9935	0.9725	0.9270	0.9668	0.9105	0.9637
	SSE	0.0038	0.0003	0.0016	0.0014	0.0007	0.0020	0.0012	0.0019	0.0016
Modified-Page	k	0.0010	0.0014	0.0011	0.0010	0.0013	0.0014	0.0018	0.0015	
	n	1.0417	1.4192	1.0977	1.0274	1.3000	1.3901	1.7539	1.5101	
	R^2	0.9745	0.9870	0.9741	0.9524	0.9784	0.9331	0.9699	0.8965	0.9582
	SSE	0.0020	0.0019	0.0003	0.0159	0.0059	0.0030	0.0020	0.0025	0.0042
Henderson & Pabis	k	0.0014	0.0020	0.0012	0.0029	0.0024	0.0014	0.0031	0.0021	
	a	0.9864	1.0118	1.000	0.9489	0.9376	0.9775	1.000	0.9739	
	R^2	0.9730	0.9870	0.9741	0.9969	0.9803	0.9275	0.9699	0.8947	0.9629
	SSE	0.0004	0.0025	0.0003	0.0036	0.0009	0.0062	0.0020	0.0018	0.0022
Two-term	k_1	0.0016	0.0029	0.0014	0.0028	0.0025	0.0019	0.0031	0.1498	
	k_2	0.0016	0.0029	0.0014	0.0028	0.0025	0.0019	0.0031	0.0021	
	a	0.5040	0.5298	0.5677	0.4864	0.5000	0.4494	0.5340	0.0277	
	b	0.5038	0.4702	0.4323	0.5687	0.5000	0.5506	0.4660	0.9723	
	R^2	0.9716	0.9859	0.9734	0.9770	0.9806	0.9331	0.9699	0.9121	0.9629
	SSE	0.0002	0.0003	0.0005	0.0014	0.0005	0.0030	0.0020	0.0017	0.0012
Verma	k	0.0016	0.0032	0.0015	0.0026	0.0021	0.0018	0.0031	0.0021	
	g	0.5045	0.0925	0.0651	0.0562	0.0249	0.0579	0.0031	0.1498	
	a	0.9920	1.0487	1.0388	1.0487	0.8930	0.9017	0.6921	0.9723	
	R^2	0.9690	0.9946	0.9861	0.9781	0.9838	0.9673	0.9699	0.9121	0.9701
	SSE	0.0004	0.0001	0.0002	0.0010	0.0005	0.0005	0.0020	0.0017	0.0007
Midilli	k	0.0027	0.0013	0.0002	0.0008	0.0063	0.0134	0.0003	0.0034	
	n	0.9128	1.3562	1.4552	1.3291	0.8072	0.6905	1.6836	1.1150	
	a	1.0000	1.0000	1.0000	1.0000	1.0000	1.0000	1.0000	1.0000	
	b	0.0000	0.0025	0.0008	0.0011	0.0000	0.0002	0.0024	0.0020	
	R^2	0.9628	0.9968	0.9706	0.9793	0.9863	0.9716	0.9666	0.9498	0.9730
	SSE	0.0006	0.0001	0.0003	0.0009	0.0003	0.0004	0.0017	0.0009	0.0007
Diffusion approach	k	0.0014	0.0029	0.0014	0.0029	0.0249	0.0078	0.0031	0.0065	
	a	1.6588	0.9225	0.5250	0.8824	0.1070	0.4260	0.5179	0.4769	
	b	0.7634	0.9994	1.0001	1.0001	0.0826	0.000	1.0016	0.000	
	R^2	0.9717	0.9858	0.9734	0.9772	0.9838	0.9740	0.9699	0.9380	0.9717
	SSE	0.0003	0.0003	0.0005	0.0008	0.0005	0.0004	0.0020	0.0012	0.0007

Table S2. Calculated values of several models of corn drying with natural zeolite.

Model		15 m/s				10 m/s				Average
		40 ℃	50 ℃	60 ℃	70 ℃	40 ℃	50 ℃	60 ℃	70 ℃	
Newton	*k*	0.0030	0.0011	0.0010	0.0010	0.0025	0.0035	0.0028	0.0028	
	R^2	0.9779	0.8695	0.9838	0.9704	0.8635	0.9827	0.9580	0.9795	0.9482
	SSE	0.0014	0.0674	0.0068	0.0370	0.0033	0.0004	0.0067	0.0021	0.0156
Page	*k*	0.0068	0.0270	0.0050	0.0009	0.0046	0.0473	0.0012	0.0024	
	n	0.8324	0.6472	0.8237	1.2482	0.8747	0.4882	1.2147	1.0418	
	R^2	0.9827	0.9350	0.9623	0.9654	0.8847	0.8849	0.9383	0.9780	0.9414
	SSE	0.0012	0.0029	0.0011	0.0021	0.0024	0.0062	0.0034	0.0012	0.0026
Modified-Page	*k*	0.0017	0.0019	0.0011	0.0018	0.0016	0.0016	0.0019	0.0018	
	n	1.7436	1.9433	1.1384	1.7550	1.5688	1.5641	1.8561	1.8358	
	R^2	0.9779	0.9036	0.9836	0.9763	0.8635	0.9800	0.9607	0.9823	0.9535
	SSE	0.0014	0.0052	0.0038	0.0011	0.0033	0.0055	0.0020	0.0004	0.0028
Henderson & Pabis	*k*	0.0018	0.0027	0.0011	0.0040	0.0025	0.0021	0.0030	0.0028	
	a	0.9827	0.9603	1.0000	0.9996	1.0000	1.0003	0.9538	0.9987	
	R^2	0.9743	0.8910	0.9838	0.9770	0.8635	0.9788	0.9589	0.9795	0.9508
	SSE	0.0128	0.0118	0.0057	0.0019	0.0032	0.0101	0.0018	0.0021	0.0062
Two-term	k_1	0.0902	0.0153	0.0018	0.0060	0.00010	0.0024	0.0034	0.0028	
	k_2	0.0026	0.000	0.0018	0.000	0.0108	0.0024	0.0034	0.0028	
	a	0.0502	0.4962	0.5676	0.6287	0.7363	0.4094	0.5341	0.7089	
	b	0.9498	0.5038	0.4324	0.3713	0.2637	0.5906	0.4659	0.2911	
	R^2	0.9845	0.9584	0.9825	0.9749	0.9039	0.9800	0.9607	0.9795	0.9656
	SSE	0.0011	0.0016	0.0004	0.0009	0.0018	0.0055	0.0020	0.0021	0.0019
Verma et al.	*k*	0.0010	0.0021	0.0020	0.0034	0.0015	0.0030	0.0034	0.0034	
	g	0.0049	0.0276	0.0050	0.0500	0.0489	0.0342	0.0034	0.0761	
	a	0.0377	0.7022	1.0022	1.0542	0.8400	0.9645	0.6956	1.0258	
	R^2	0.9799	0.9516	0.9821	0.9729	0.9130	0.9823	0.9607	0.9794	0.9652
	SSE	0.0065	0.0021	0.0004	0.0017	0.0015	0.0006	0.0020	0.0006	0.0019
Midilli et al.	*k*	0.0068	0.0006	0.0004	0.0009	0.0384	0.0042	0.0025	0.0025	
	n	0.8324	1.5971	1.3957	1.4481	0.5413	0.9904	1.0716	1.0366	
	a	1.0000	1.0000	1.0000	1.0000	1.0000	1.0000	1.0000	1.0000	
	b	0.0000	0.0027	0.0009	0.0024	0.0008	0.0005	0.0001	0.0001	
	R^2	0.9827	0.9157	0.9853	0.9750	0.8490	0.9841	0.9541	0.9783	0.9530
	SSE	0.0012	0.0045	0.0003	0.0011	0.0028	0.0007	0.0021	0.0012	0.0018
Diffusion approach	*k*	0.0030	0.0038	0.0018	0.0022	0.0025	0.0024	0.0651	0.0028	
	a	1.4709	1.0000	0.5251	0.7449	1.0000	1.0000	0.0831	0.5326	
	b	1.0000	1.0000	1.0000	0.9995	1.0000	1.0000	0.0448	1.0001	
	R^2	0.9779	0.9036	0.9825	0.9744	0.8635	0.9800	0.9775	0.9795	0.9549
	SSE	0.0014	0.0052	0.0004	0.0086	0.0032	0.0055	0.0006	0.0021	0.0034

Table S3. Calculated values of several models of corn drying with silica gel.

Model		15 m/s				10 m/s				Average
		40 ℃	50 ℃	60 ℃	70 ℃	40 ℃	50 ℃	60 ℃	70 ℃	
Newton	k	0.0021	0.0024	0.0035	0.0017	0.0009	0.0039	0.0034	0.0023	
	R^2	0.9721	0.9861	0.8423	0.9102	0.9677	0.9736	0.9700	0.9869	0.9511
	SSE	0.0124	0.0027	0.0069	0.0256	0.0069	0.0017	0.0019	0.0040	0.0077
Page	k	0.0011	0.0007	0.0605	0.0098	0.0001	0.0301	0.0109	0.0017	
	n	1.2027	1.2841	0.4583	0.7827	1.6379	0.6074	0.7709	1.1032	
	R^2	0.9614	0.9783	0.9519	0.9504	0.9678	0.9755	0.9886	0.9838	0.9697
	SSE	0.0024	0.0013	0.0016	0.0016	0.0008	0.0011	0.0004	0.0009	0.0013
Modified-Page	k	0.0014	0.0017	0.0017	0.0018	0.0010	0.0020	0.0018	0.0017	
	n	1.4416	1.7067	1.7000	1.8330	0.9572	1.9675	1.8420	1.6679	
	R^2	0.9721	0.9865	0.8323	0.9286	0.9677	0.9736	0.9700	0.9889	0.9525
	SSE	0.0124	0.0005	0.0118	0.0026	0.0069	0.0017	0.0019	0.0005	0.0048
Henderson & Pabis	k	0.0021	0.0028	0.0022	0.0029	0.0014	0.0026	0.0028	0.0028	
	a	0.9955	0.9832	1.0000	0.9428	1.0000	0.8936	0.9174	1.0000	
	R^2	0.9721	0.9808	0.8199	0.9242	0.9659	0.9675	0.9670	0.9889	0.9483
	SSE	0.0117	0.0006	0.0229	0.0024	0.0018	0.0030	0.0010	0.0005	0.0055
Two-term	k_1	0.0052	0.0182	0.0126	0.0149	0.0021	0.0025	0.0219	0.0036	
	k_2	0.0001	0.0018	0.0001	0.0001	0.0021	0.0391	0.0030	0.0001	
	a	0.7296	0.1513	0.5373	0.4896	0.1201	0.7765	0.0848	0.9436	
	b	0.2704	0.8487	0.4627	0.5104	0.8799	0.2235	0.9152	0.0564	
	R^2	0.9851	0.9704	0.9556	0.9667	0.9629	0.9685	0.9813	0.9906	0.9726
	SSE	0.0005	0.0012	0.0012	0.0018	0.0012	0.0013	0.0007	0.0004	0.0010
Verma et al.	k	0.0010	0.0032	0.0020	0.0037	0.0022	0.0035	0.0023	0.0033	
	g	0.0049	0.0562	0.0479	1.3000	0.0800	0.0596	0.0415	1.3000	
	a	0.2269	1.0506	0.7384	0.9710	1.0390	0.9374	0.0808	0.9952	
	R^2	0.9835	0.9874	0.9632	0.9356	0.9797	0.9856	0.9766	0.9899	0.9752
	SSE	0.0006	0.0005	0.0014	0.0016	0.0003	0.0006	0.0010	0.0004	0.0008
Midilli et al.	k	0.0015	0.0012	0.0050	0.0012	0.0011	0.0074	0.0067	0.0024	
	n	1.2916	1.4035	1.1570	1.4923	1.3462	0.8720	0.8760	1.0446	
	a	1.0000	1.0000	1.0000	1.0000	1.0000	1.0000	1.0000	1.0000	
	b	0.0015	0.0023	0.0025	0.0035	0.0023	0.0001	0.0001	0.0001	
	R^2	0.9875	0.9839	0.9728	0.9299	0.9735	0.9833	0.9827	0.9878	0.9752
	SSE	0.0006	0.0006	0.0008	0.0028	0.0006	0.0008	0.0006	0.0003	0.0009
Diffusion approach	k	0.0032	0.0034	0.0160	0.0034	0.0021	0.0039	0.0415	0.0023	
	a	1.4690	1.0000	0.4361	0.7557	1.0000	1.0000	0.1992	1.0000	
	b	1.0000	1.0000	0.0001	1.0001	1.0000	1.0000	0.0548	1.0000	
	R^2	0.9786	0.9864	0.9750	0.9286	0.9629	0.9736	0.9766	0.9870	0.9711
	SSE	0.0010	0.0008	0.0013	0.0026	0.0012	0.0017	0.0010	0.0040	0.0017